Journal of Statistical Physics, Vol. 80, Nos. 5/6, 1995

Ising-Type Transitions in Coupled Map Lattices

C. Boldrighini,[1] L. A. Bunimovich,[2] G. Cosimi,[1] S. Frigio,[1] and A. Pellegrinotti[3]

Received August 5, 1994; final March 22, 1995

We study, by means of computer simulations, some models of coupled map lattices (CML) with symmetry, subject to diffusive nearest neighbor coupling, with the purpose of providing a better understanding of the occurrence of Ising-type transitions of the type found by Miller and Huse. We argue, on the basis of numerical evidence, that such transitions are connected to the appearance of a minimum in the Lyapunov dimension of the system as a function of the coupling parameter. Two-dimensional CMLs similar to the one in Miller and Huse, but with no minimum in the Lyapunov dimension plot, have no Ising transition. The condition seems to be necessary, though by no means sufficient. We also argue, relying on the analysis of Bunimovich and Sinai, that coupled map lattices should behave differently, with respect to dimension, than Ising models.

KEY WORDS: Coupled map lattices; Ising-type transitions; Lyapunov dimension; chaotic systems.

0. INTRODUCTION

Studies of order and chaos and of transitions between these types of behavior in finite-dimensional dynamical systems (also called sometimes "point" or nonextended) have led to a rich self-consistent theory.[1-3] This was mainly due to the elaboration of exact (mathematical) definitions of such statistical properties as ergodicity, weak mixing, mixing, rate of decay of correlations, Bernoulli property, etc., and of such topological (or geometrical) objects as homoclinic and heteroclinic points, horseshoes,

Dedicated to Yakov Grigorievich Sinai on his 60th birthday.

[1] Dipartimento di Matematica e Fisica, Università di Camerino, 62032 Camerino, Italy.
[2] Center for Dynamical Systems and Nonlinear Studies, Georgia Institute of Technology, Atlanta, Georgia 30332.
[3] Dipartimento di Matematica, Terza Università di Roma, 00146 Rome, Italy.

822/80/5-6-17

etc., that ensure some kind of complex "behavior" of the corresponding dynamical systems.

The modern theory of chaos relies essentially on examples of model systems for which these properties or objects can be rigorously proven to exist. The theory of bifurcations provides the tools for studying transitions between different types of local or global behavior in dynamical systems.[4,5] The results of the theory have found extensive applications and have even allowed "scenarios of transitions to turbulence"[6] where by "turbulence" one means basically some kind of chaotic motion in time only.

The general notions of turbulence, space-time chaos, coherent structures, and intermittency have long been applied in analyzing experimental results of the motion of extended media, especially fluid flows, with remarkable success. An extensive theory has also been developed,[7–9] but, surprisingly, without exact definitions of some basic concepts and phenomena. This theory is essentially a collection of some explicit phenomenological results concerning special classes of models of extended media (extended dynamical systems). As examples we can quote the celebrated Kolmogorov theory of homogeneous isotropic turbulence[7] and the numerous works on the theory of hydrodynamic stability.[10]

The situation began to change quite recently with the introduction of new classes of extended dynamical systems that have been called coupled map lattices (CMLs)[11]. These systems describe the evolution of a finite or infinite number of interaction "point" (finite-dimensional) dynamical systems located at the sites of some lattice in a "physical" space. Thus the CMLs form a class of coupled oscillator systems in which each oscillator is characterized not only by its (internal) state, but also by its (fixed) coordinate in space. Such systems were considered before the name coupled map lattices was invented.[12] By introducing a general "abstract" class of extended dynamical systems it became possible to give a precise definition of the phenomenon of space-time chaos[13] and to prove its existence in some classes of CMLs.[14] Moreover, in ref. 13 the first definition of coherent structure was given, and it was proposed that such structures can emerge in CMLs if the strength of the space interaction (order parameter) increases.

The definition of coherent structure in ref. 13 relies on a exact representation of extended dynamical systems (CMLs) as lattice spin systems of statistical mechanical type. The existence of space-time chaos in CMLs was proven for weakly interacting, strongly chaotic (local) dynamical systems on the lattice.[13,17,18] In ref. 13 this result was obtained by connecting space-time chaos to the absence of phase transitions in lattice spin systems of statistical mechanical type. That is, only one

phase (space-time chaos) emerges in the range of weak space interactions that corresponds to the range of high temperatures in a dual lattice spin system. It is important to observe that while the one-dimensional lattice spin systems correspond to finite-dimensional (nonextended) dynamical systems (see, e.g., refs. 19 and 20), the dimension of the spin systems corresponding to CMLs equals at least two. Thus in such systems phase transitions can be expected to occur for one-dimensional lattices also.

The emergence of new phases can be naturally interpreted as the appearance of coherent structures in the corresponding extended dynamical system (CML). Such phase transitions, as usual for dynamical systems, can be described by bifurcations that appear when the parameters of the space interaction vary, and produce a transition from space-time chaos to some more organized type of motion. These ideas were confirmed by various computer simulations[21–24] and some analytical studies.[26, 27]

One should note, however, that the transitions found, for example, in refs. 21–24 for CMLs of logistic maps interacting on the one-dimensional lattice do not resemble the phase transitions known in statistical mechanics. This fact is not surprising, since the lattice spin systems that correspond to CMLs are essentially nonisotropic, as one of the dimensions corresponds to the dynamics in time and all other dimensions to space. A natural question is, however, whether or not CMLs can show the same type of phase transitions as the classical models of statistical physics, and first of all as the Ising model.

A positive answer to this question was obtained recently by Miller and Huse,[28] who have found Ising-type phase transitions in a two-dimensional square lattice of diffusively coupled piecewise linear expanding maps, symmetric with respect to reflection. The one-dimensional CML of the same local maps with analogous coupling does not show such types of transitions. This result was used in ref. 28 to argue that phase transitions analogous to those in the lattice models of statistical physics can occur in CMLs, but again starting with dimension 2. It would seem that the difference between extended and nonextended dynamical systems pointed out in ref. 13 does not exist for one-dimensional CMLs, or is anyhow inessential.

The aim of the present paper is to provide a deeper understanding of Ising-type transitions for CMLs, by pointing out some characteristic features which are due to the fact that such systems are extended in space and time. We argue that in order to have such transitions there should be some "balance" between the local production of chaos (nonlinearity) and the diffusion strength (dissipation), which can be expressed by the behavior of the Lyapunov dimension. The balance that is needed seems to correspond to the presence of a minimum of the Lyapunov dimension as

a function of the coupling (diffusive) strength. We show that two-dimensional lattices of coupled maps with "Ising symmetry" very similar to the one considered in ref. 28, but such that the Lyapunov dimension does not decrease by increasing the coupling parameter, can fail to have Ising-type (and even any "interesting") phase transitions.

We believe that one-dimensional CMLs, as systems which are extended in time and space, should also provide Ising-type phase transitions, though we are unable for the moment to provide numerical evidence to that effect. We briefly report, however, the numerical results for a one-dimensional CML which shows the appropriate behavior of the Lyapunov dimension, and seems to get "close" to an Ising-type transition. It can be considered as a starting point for further efforts to find evidence of Ising-type transitions in one-dimensional CMLs.

The search for more stringent conditions on the appearance of Ising-type transitions would require the study of the leading modes, and is a subject for further study.

The paper is divided into three sections. The first section is devoted to the description of the models. In the second section we report the computer results on the three-piece map studied in ref. 28, with special attention to the Lyapunov dimension and to space-inhomogeous states. In the third section we report results on models that do not exhibit Ising-type transitions.

Computation of the Lyapunov exponents has been done along the lines proposed in ref. 32.

1. DESCRIPTION OF THE MODEL

We consider CMLs on a finite d-dimensional square lattice generated by diffusion-type coupling of local (point) dynamical systems. The local systems always belong to the class of one-dimensional maps f of the interval $I=[-1, 1]$ into itself with the further property that f is continuous and piecewise linear.

The phase space of our CML is

$$\Omega_N^{(d)} = \{x = \{x_{\mathbf{k}} \in I: \mathbf{k} \in (\mathbb{Z}_N)^d\}\} \tag{1.1}$$

where $\mathbb{Z}_N = \mathbb{Z}/(N\mathbb{Z})$ denotes the integers considered modulo N. On $\Omega_N^{(d)}$ we consider the maps Φ_ε and F with values in $\Omega_N^{(d)}$ and defines as

$$(\Phi_\varepsilon x)_{\mathbf{k}} = (1-\varepsilon)\, x_{\mathbf{k}} + \varepsilon \sum_{\mathbf{j} \in (\mathbb{Z}_N)^d} a_{\|\mathbf{j}-\mathbf{k}\|} x_{\mathbf{j}} \tag{1.2a}$$

$$F_{\mathbf{k}}(x) = f(x_{\mathbf{k}}) \tag{1.2b}$$

Here $\varepsilon \in (0, 1]$, $\|\mathbf{j}\| = \sum_{j=1}^{d} |j_l|$, where j_l are the components of the vector $\mathbf{j}$, and $\sum_j a_{\|\mathbf{j}\|} = 1$.

The dynamics of the coupled map lattice is given by the composition

$$H_\varepsilon = \Phi_\varepsilon \circ F \tag{1.3}$$

i.e., by the successive action of the local map F and the coupling Φ_ε. Clearly

$$(H_\varepsilon x)_{\mathbf{k}} = (1-\varepsilon) f(x_{\mathbf{k}}) + \varepsilon \sum_{\mathbf{j} \in (\mathbb{Z}_N)^d} a_{\|\mathbf{j}-\mathbf{k}\|} f(x_{\mathbf{j}}) \tag{1.4}$$

The CMLs under consideration can be described as an array of one-dimensional continuous piecewise linear maps, on the periodic d-dimensional lattice $(\mathbb{Z}_N)^d$, which interact diffusively.

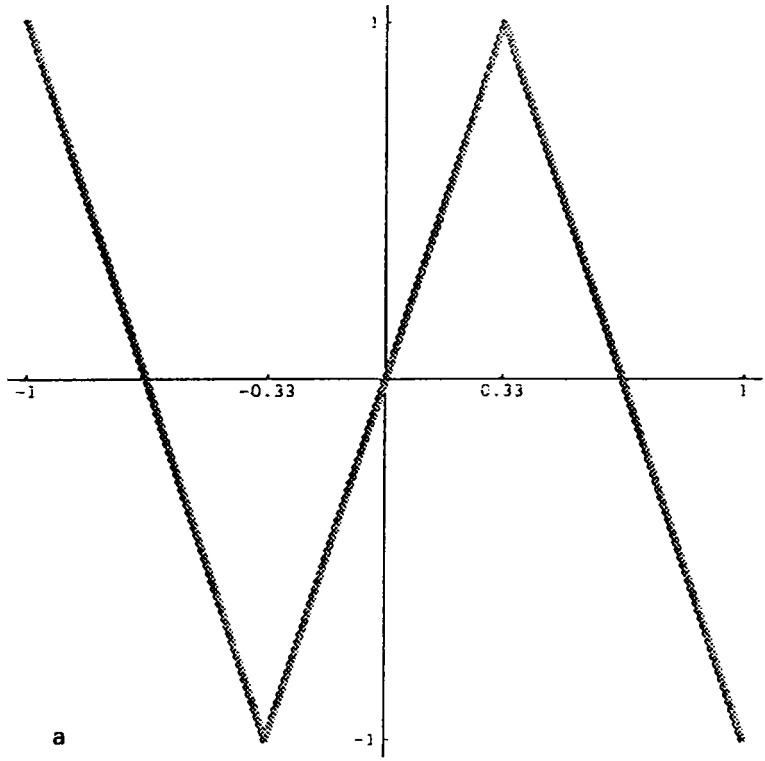

Fig. 1. The three maps studied in this paper. (a) The map denoted in the text f_3, (b) f_5, and (c) f.

We consider CMLs with nearest neighbor coupling, i.e.,

$$(\Phi_\varepsilon x)_{\mathbf{k}} = (1-\varepsilon)\, x_{\mathbf{k}} + \frac{\varepsilon}{2d} \sum_{\|\mathbf{j}-\mathbf{k}\|=1} x_{\mathbf{j}} \tag{1.5}$$

In fact most numerical studies of CMLs were done for nearest neighbor coupling.

The CML corresponding to the map f in dimension d and to the coupling (1.5) will be denoted by $H^{(d)}_{f,\varepsilon}$.

We report computer simulations for the three maps shown in Figs. 1a–1c. They are denoted as f_3, f_5 and f. The maps f_3 and f_5 have a slope of constant absolute value, equal to 3 and 5, respectively. They can be considered as a generalization of the popular "tent maps." Lattices of tent maps with nearest neighbor diffusive coupling were considered in ref. 31. No interesting phase transitions, and in particular no Ising-type transitions, were found.

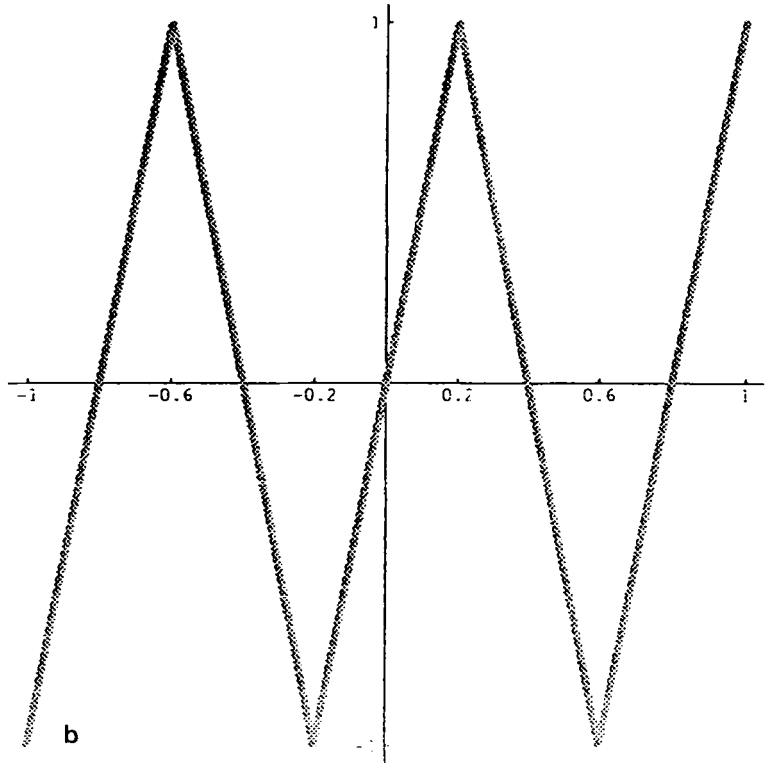

Fig. 1 (*continued*)

Maps similar to f_3 and f_5 were studied, with different aims, in refs. 29 and 30.

The linearization of the maps $H^{(d)}_{f_s,\varepsilon}$, $s=3, 5$, at a point $x=\{x_i\}_{i\in(\mathbb{Z}_N)^d}$ has a particularly simple expression. For $d=1$ it is expressed by the matrix $sA(x)$, with

$$A(x)=\begin{pmatrix} (1-\varepsilon)\,\xi_0 & \frac{1}{2}\varepsilon\xi_1 & 0 & \cdots & 0 & \frac{1}{2}\varepsilon\xi_{N-1} \\ \frac{1}{2}\varepsilon\xi_0 & (1-\varepsilon)\,\xi_1 & \frac{1}{2}\varepsilon\xi_2 & \cdots & 0 & 0 \\ \cdots & \cdots & \cdots & \cdots & \cdots & \cdots \\ \frac{1}{2}\varepsilon\xi_0 & 0 & 0 & \cdots & \frac{1}{2}\varepsilon\xi_{N-2} & (1-\varepsilon)\,\xi_{N-1} \end{pmatrix} \tag{1.6}$$

Here $\xi_k=\xi_k(x)=\operatorname{sign}(f'(x_k))$ is the sign of the derivative of the map computed at the point x_k. A similar formula holds for $d>1$, with the only

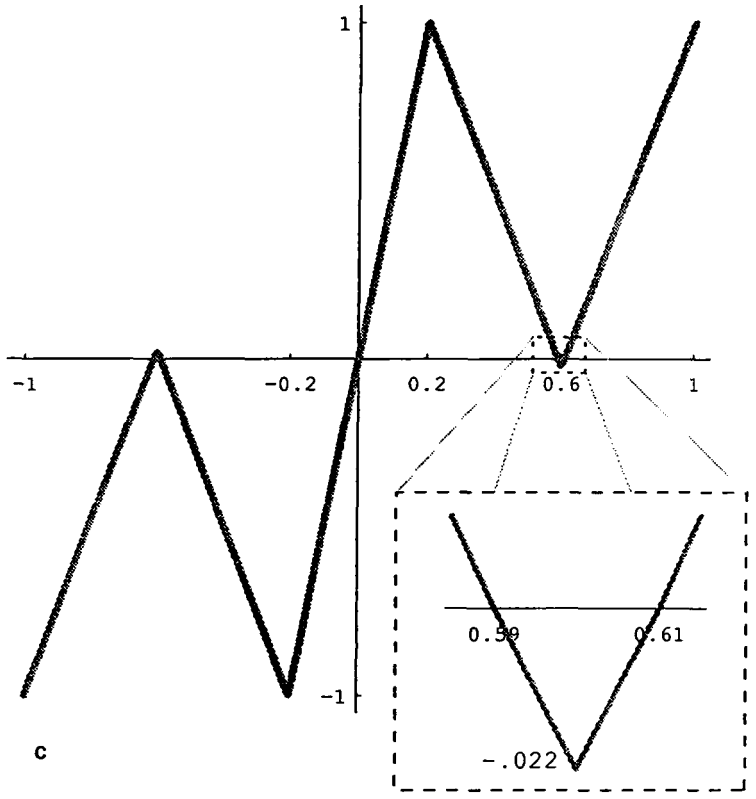

Fig. 1 (*continued*)

difference that the entries of A will be labeled by the points of $(\mathbb{Z}_N)^d$. Such formulas simplify the computation of the Lyapunov exponents.

We usually choose the initial data $x_{\mathbf{k}}(0)$, $\mathbf{k} \in (\mathbb{Z}_N)^d$, as realizations of independent (in $\mathbf{k}$) random variables. In most cases they are realizations of the same random variable ξ, uniformly distributed in the interval $(-1, 1)$, a situation which we describe concisely by the expression "symmetric random initial data." Sometimes the random variable ξ is uniformly distributed in $(0, 1)$ or in $(-1, 0)$, in which case we speak of positive or negative random initial data. The adjective random may be omitted.

For the space average (which is a natural empirical order parameter) and the empirical dispersion we shall use the notation

$$X(t) = \frac{1}{N^d} \sum_{\mathbf{k}} x_{\mathbf{k}}(t) \tag{1.7}$$

$$D(t) = \frac{1}{N^d} \sum_{\mathbf{k}} [x_{\mathbf{k}}(t) - X(t)]^2 \tag{1.8}$$

2. THE CML $H^{(2)}_{f_3,\epsilon}$

The CML $H^{(2)}_{f_3,\varepsilon}$ is essentially the same as the one studied in ref. 28 and it is known from that paper that it exhibits Ising-type transitions. Our results locate the critical value ε_c around the value 0.81, in accordance with the result of ref. 28.

Most simulations were done on the square lattice $N \times N$, for $N = 100$, with periodic boundary conditions. N is, however, always indicated in the figure captions.

2.1. Subcritical ϵ

For $\varepsilon < \varepsilon_c$ there is a unique chaotic regime, and the attractor is symmetric with respect to the origin (under the exchange $x \to -x$). $X(t)$ tends, as $t \to \infty$, to values of the order $1/N$ exponentially fast. $D(t)$ behaves similarly and tends to a value which is around 0.25.

Figure 2a shows the behavior of $X(t)$ for $\varepsilon = 0.3$, for t up to 5 units and positive random initial data. Figure 2b shows the occupation number histogram for large time ($t = 10^4$). The histogram is constructed by dividing the interval I into small cells (cell positions between -1 and 1 are on the horizontal axis), and reporting on the vertical axis the occupation number of each cell, i.e., how many variables $x_{\mathbf{k}}$ take values in the cell.

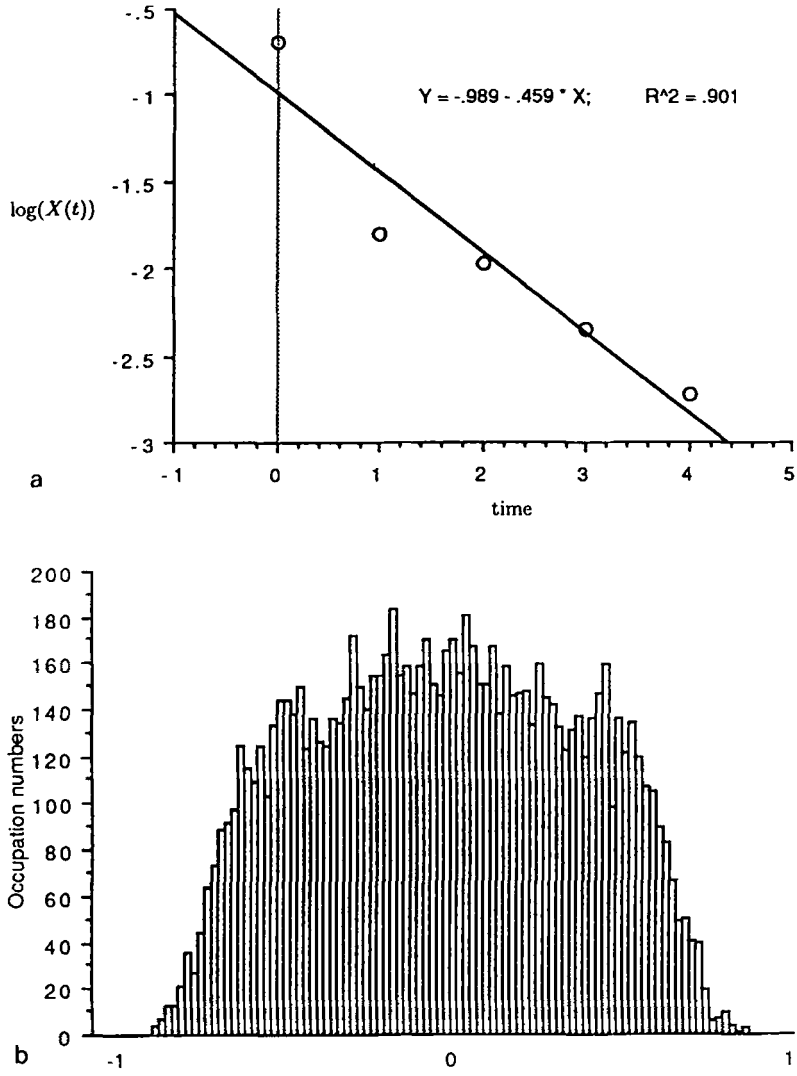

Fig. 2. The CML with map f_3 on the 100×100 periodic square lattice at $\varepsilon = 0.3$. (a) The falloff of $\log X(t)$ in the first few time units for positive random initial data. (b) The occupation number histogram (described in the text) at a given large time.

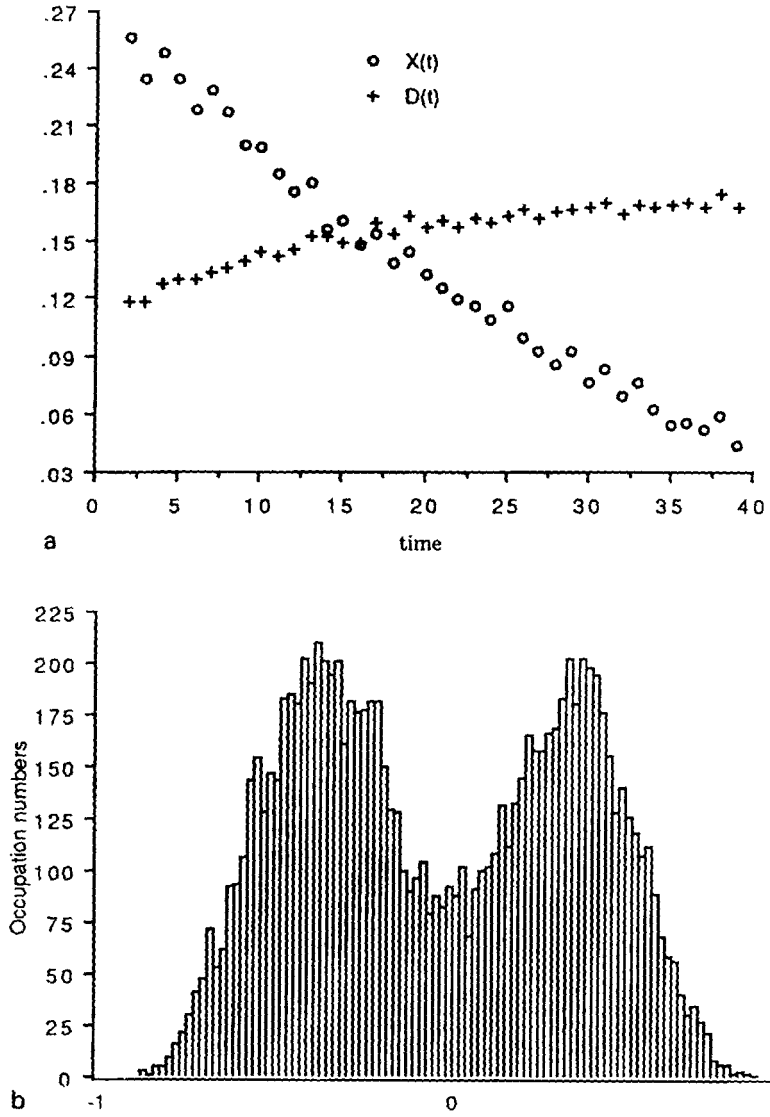

Fig. 3. The CML with map f_3 on the 100×100 periodic square lattice at $\varepsilon = 0.6$. (a) The behavior of $X(t)$ and $D(t)$ up to 40 time units for positive random initial data. (b) The occupation number histogram at a given large time.

For values of ε around 0.4 some change takes place. The occupation number histogram gets depressed in the middle, forming a marked two-bump profile, with maxima around ± 0.4. Moreover, $X(t)$ relaxes to 0 very slowly, apparently as an inverse power.

Figure 3a shows the behavior of $X(t)$ and $D(t)$ for positive random initial data and $\varepsilon = 0.6$. Figure 3b shows the occupation number histogram at $t = 10^4$.

The chaotic regime, with a space-homogeneous stationary state, persists up to $\varepsilon \approx 0.8$. As ε grows, the two-bump profile of the occupation number histogram, with peaks around ± 0.4, gets enhanced.

2.2. The Transition and the Two-Phase Region

We have not examined in detail the behavior near the critical point, as it was extensively done in ref. 28, where the critical exponents were also computed. The interested reader is referred to that paper. We only report in Fig. 4 the behavior of the space average $X(t)$ for $\varepsilon = 0.80$. The regime of large oscillations around zero is of course due to the fact that the correlation length is no longer negligible with respect to N.

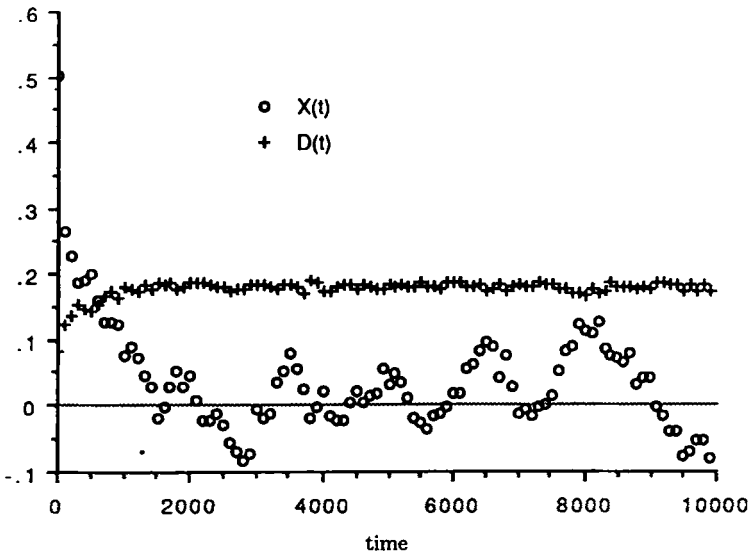

Fig. 4. The CML with map f_3 on the 100×100 periodic square lattice at $\varepsilon = 0.8$: behavior of $X(t)$ and $D(t)$ up to 10,000, for positive random initial data.

For $\varepsilon > \varepsilon_c$ two symmetric translation-invariant states appear, which we denote by $\mu_\pm$, and are related by the symmetry $x \to -x$. For symmetric random initial data the average $X(t)$, after some oscillations, tends in most cases to a definitely nonzero asymptotic value, which can be $\pm c$, with c close to 0.4. The reason why it does not tend always to the values corresponding to the states $\mu_\pm$ is the presence of space-nonhomogeneous states, which are discussed below. The time averages of the variables $x_\mathbf{k}$ are independent of $\mathbf{k}$ and close, for large times, to $\pm c$ (for $\mu_\pm$, respectively).

Figure 5a gives the behavior of $X(t)$ and $D(t)$ for symmetric random initial data and $\varepsilon = 0.84$. One can see that, as time grows, $X(t)$ departs from 0 and assumes a value around $+c$.

Figure 5b gives the density plots on the lattice $(\mathbb{Z}_N)^2$ at a time $(t = 10^4)$ much larger than the relaxation time, for a run which tends to the state μ_-. The plot is obtained as follows: at each site $\mathbf{k} \in (\mathbb{Z}_N)^2$ a small square is colored with different shades of grey, according to the value of x_k, varying from black for $x_k = -1$ to white for $x_k = 1$.

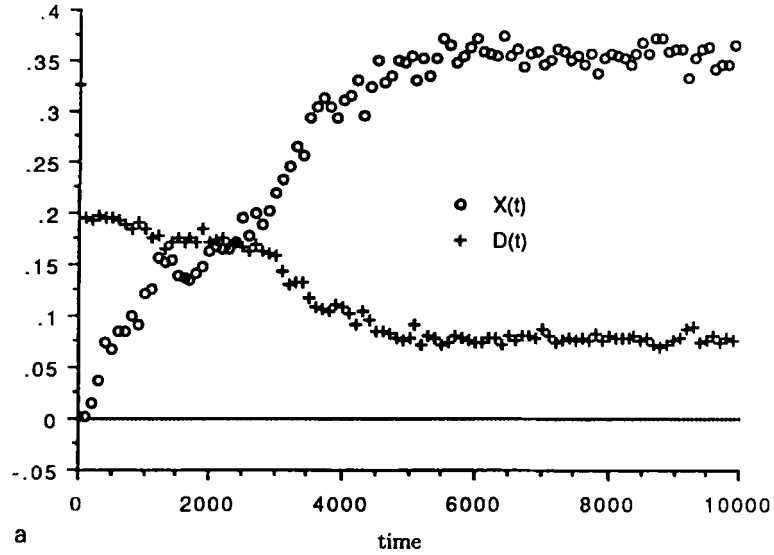

Fig. 5. The CML with map f_3 on the 100×100 periodic square lattice at $\varepsilon = 0.84$. (a) The behavior of $X(t)$ and $D(t)$ up to $t = 10,000$, for symmetric random initial data. (b) The density plot on the square lattice for another run with symmetric random initial data, which tends to the attractor corresponding to μ_-. The plot is taken at time $t = 10,000$, and is obtained by coloring the unit squares with centers at the lattice sites with different shades of grey, going from white for $x_\mathbf{k} = 1$ to black for $x_\mathbf{k} = -1$.

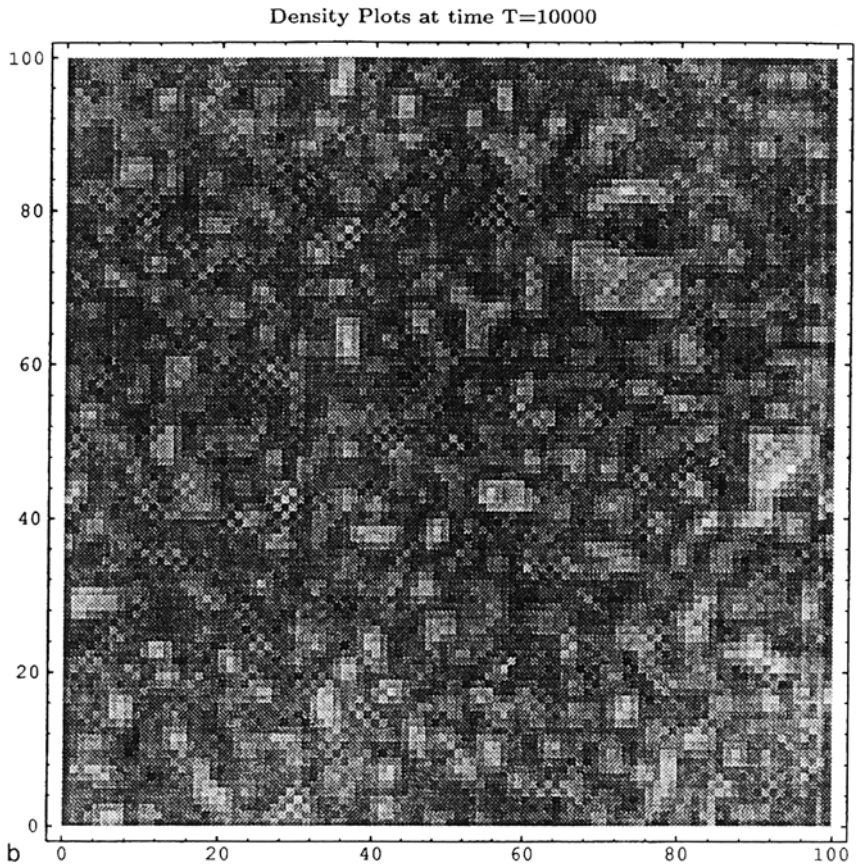

Fig. 5 (*continued*)

2.3. Lifetime of a Strip

For $\varepsilon > \varepsilon_c$ some runs tend rather slowly to the pure phases, going through some nonhomogeneous situations in which the two phases $\mu_\pm$ coexist in two regions separated by interface lines which are roughly parallel to one of the coordinate axes. In order to understand how long they actually persist, we made a computer simulation as follows. We take random initial data that are positive for $k_2 \in (N/2, N]$ and negative for $k_2 \in (0, N/2]$, a situation which leads very quickly to two horizontal strips with different phases. The lifetime of the strips is computed by stopping the run at the first time $T(N)$ when the absolute value of the average $X(t)$ gets

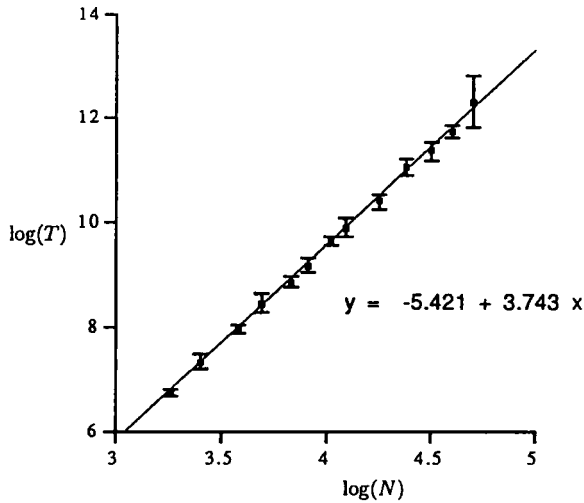

Fig. 6. Behavior of the lifetime of a strip of width $N/2$ as a function of N. The error bars correspond to two standard errors, and different values of N have different statistics, going from a sample of 400 to 15 (for $N=110$).

over 0.3. For the value $\varepsilon=0.94$ that we consider the average of $X(t)$ lies in absolute value between 0.38 and 0.39.

Figure 6 shows the plot of $\log[T(N)]$ versus $\log N$. A behavior of the type $T(N) \asymp \text{const } N^{\alpha}$ with $\alpha \approx 3.75$ seems to fit well. For the Ising model with Glauber dynamics one would expect $\alpha=3$, hence our results indicate that that for our *CML* the coexistence of phases is more persistent.

The situation is not entirely clear, as, for instance, a behavior of $\log[T(N)]$ of the type $c_1+c_2N^{\gamma}$, where c_1 and c_2 are constants and γ is between 1/4 and 1/2 (for instance, $-1.7+3N^{1/3}$) fits our data almost as well. More work, and more data, are needed in order to get a better understanding of this important point.

The two homogeneous phases $\mu_{\pm}$ persist up to $\varepsilon=1$.

2.4. Behavior of the Lyapunov Dimension

Figure 7 shows the behavior of the Lyapunov dimension as a function of ε. We extend for convenience the definition of Lyapunov dimension to the case when there are no negative Lyapunov exponents, by setting it equal to the full dimension. One can clearly see that there is a neat minimum near the critical value ε_c.

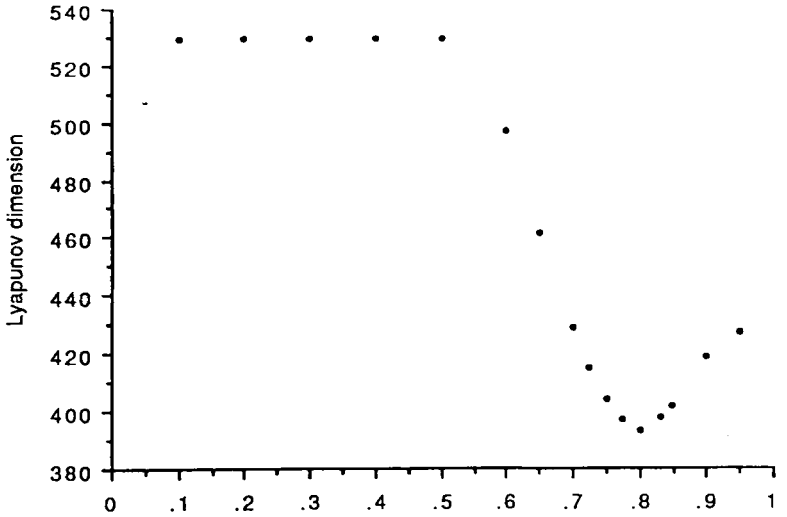

Fig. 7. The CML with map f_3 on the 23×23 periodic square lattice: Lyapunov dimension as a function of ε.

3. EXAMPLES OF MAPS THAT DO NOT HAVE ISING-TYPE TRANSITIONS

3.1. The CML $H^{(2)}_{f_5,\epsilon}$

Though two-dimensional, this map does not show any significant transition, in particular no Ising-type transitions. Positive and negative values of the spins seem to be present in equal amounts in the asymptotic (in time) states obtained both from negative and from positive random initial data. $X(t)$ relaxes to values close to 0 for all initial data.

Figure 8a shows the behavior of $X(t)$ and $D(t)$ at $\varepsilon = 0.8$, for positive random initial data. For other values of ε the behavior is similar.

Figure 8b gives the density plots at $t = 10^4$ for the same run. The two bumps in the occupation number histogram also never appear. Figure 8c shows the histogram again at $\varepsilon = 0.8$. As ε increases from 0 to 1 the occupation number plot only changes in that the peak around 0 becomes sharper. Also the density plots differ only in that for small ε they show a "finer grain."

The plot of the Lyapunov dimension as a function of ε is completely flat, i.e., the Lyapunov dimension is equal to the full dimension N^2 for all $\varepsilon \in [0, 1]$.

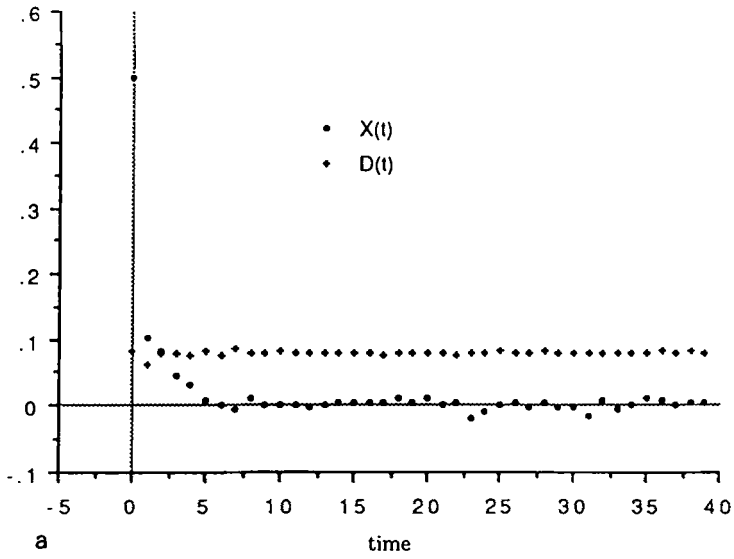

Fig. 8. The CML with map f_5 on the 100×100 periodic square lattice at $\varepsilon = 0.8$. (a) The behavior of $X(t)$ and $D(t)$ up to 40 time units for positive random initial data. (b) the density plot at time $t = 10,000$. (c) The corresponding occupation number histogram.

3.2. The CML $H^{(1)}_{f,\varepsilon}$

The map f is shown in Fig. 1c. We give here for better reference its analytic expression (only for the positive half-interval, as the map is antisymmetric). For $D = 1/100$ and $K = -1/45$ we have

$$f(x) = \begin{cases} 5x & 0 \leqslant x \leqslant \frac{1}{5} \\ -\frac{5}{2-5D}x + \frac{3-5D}{2-5D} & \frac{1}{5} \leqslant x \leqslant \frac{3}{5} - D \\ \frac{K}{D}x + K\left(1 - \frac{3}{5D}\right) & \frac{3}{5} - D \leqslant x \leqslant \frac{3}{5} \\ -\frac{K}{D}x + K\left(1 + \frac{3}{5D}\right) & \frac{3}{5} \leqslant x \leqslant \frac{3}{5} + D \\ \frac{5}{2-5D}x - \frac{3+5D}{2-5D} & \frac{3}{5} + D \leqslant x \leqslant 1. \end{cases} \tag{3.1}$$

Computer simulations are done for values of N ranging between 500 and 2000.

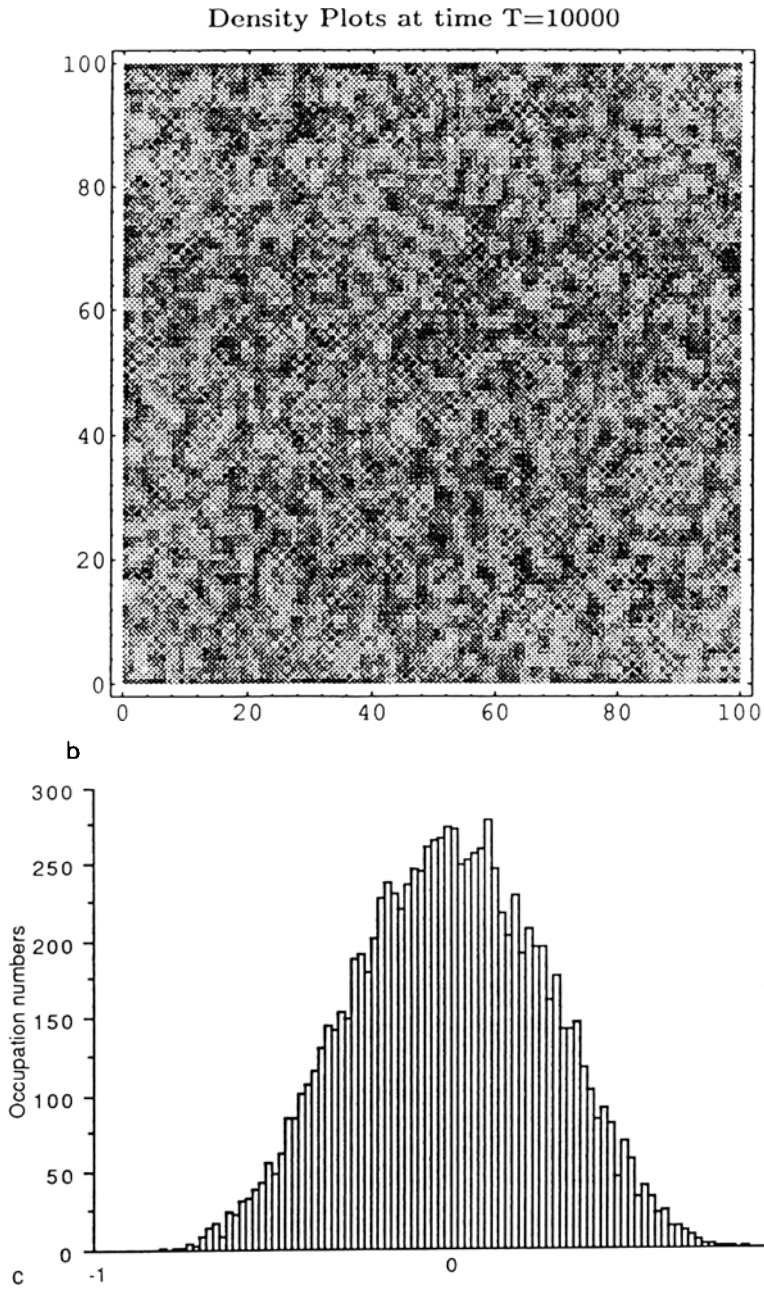

Fig. 8 (*continued*)

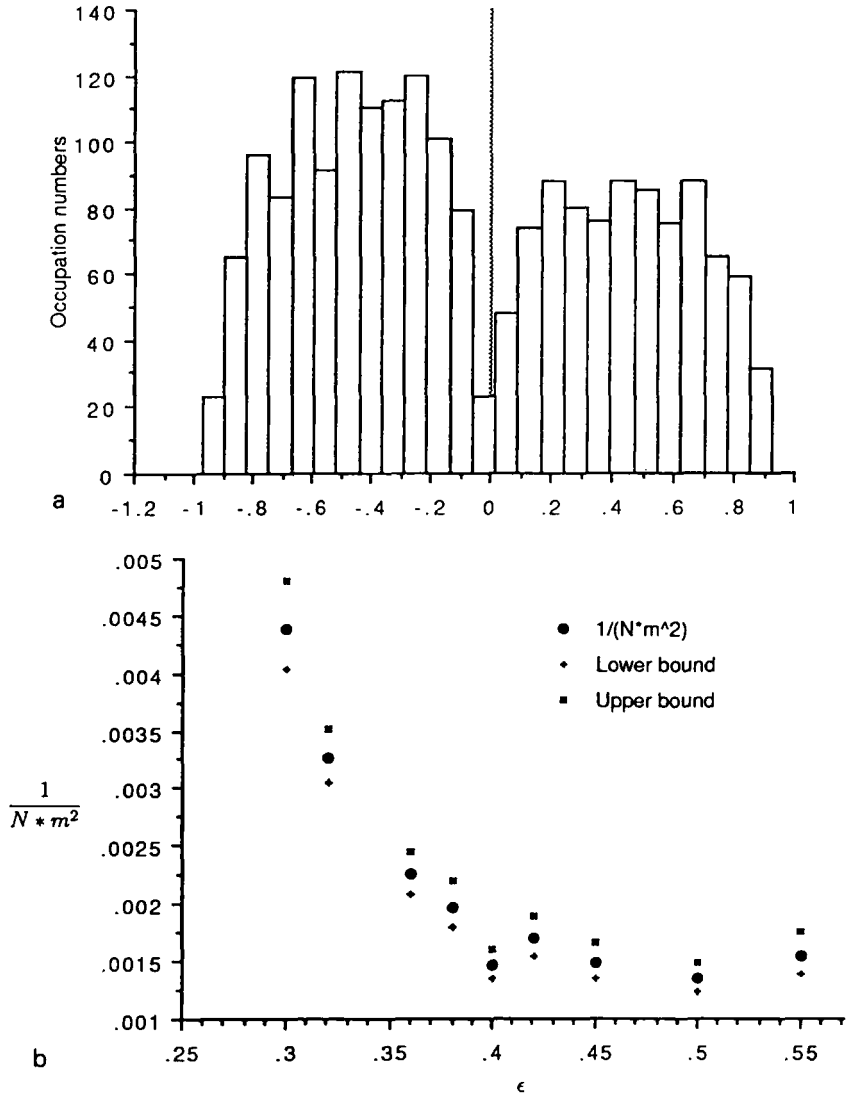

Fig. 9. The one-dimensional CML with map f. (a) The typical asymptotic (in time) occupation number histogram. The length of the periodic lattice is $N = 2000$, and $\varepsilon = 0.15$. (b) The behavior of Nm^2 as a function of ε, where m^2 is the average of the square of the magnetization M, defined as $M = (1/N) \sum_{k=1}^{N} \text{sign } x_k$, over a sample of 100 independent runs with symmetric random initial data. The upper and lower bounds correspond to the standard error of m^2. The time at which the magnetization is computed and the value of N are chosen for each ε separately. We first compute the asymptotic behavior in t for fixed N and then increase N until an asymptotic behavior is reached. (c) The Lyapunov dimension as a function of ε for $N = 500$.

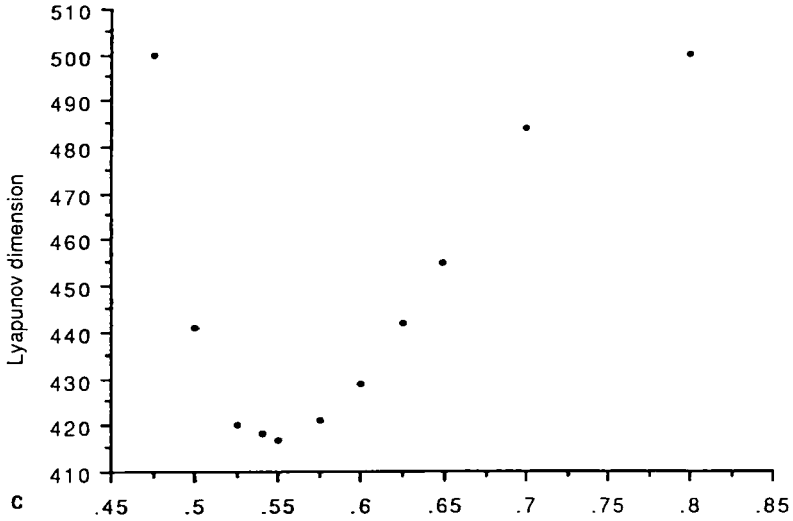

Fig. 9 (*continued*)

This particular CML was considered to be a good candidate for a one-dimensional CML exhibiting Ising-type transitions. However, it appears that it only gets "very close" to that. For small ε there is a unique chaotic regime, the attractor is symmetric for sign change, and there are no bumps in the occupation number histogram. As ε increases, the two-bump structure appears, as shown in Fig. 9a, and relaxation is slow. However, it appears that the correlation length gets only very long (of the order of thousand of units), but does not diverge. Figure 9b shows the behavior of the inverse of $N\langle m^2\rangle$ as a function of ε, where $m=(1/N)\sum_k x_k$ is the average magnetization, and the average $\langle\cdot\rangle$ is taken over a sample of 100 independent runs. The sample length N is adjusted in such a way that it is always larger than the double of the correlation length. This is checked by looking at the stabilization of $N\langle m^2\rangle$ when N is increased.

On the basis of the behavior of the Lyapunov dimension, shown by Fig. 9c, one would expect a critical value around in the range $\varepsilon\in(0.55, 0.6)$. However, Fig. 9b shows that the function $(N\langle m^2\rangle)^{-1}$ at first decreases in the right way, but then fails to tend to 0, as ε grows and gets near to where the critical value should be.

4. CONCLUSIONS

The results of the present paper show that the "Ising-type symmetry" of the local maps does not ensure the existence of Ising-type phase

transitions in the corresponding CML with nearest neighbor diffusive coupling, in contrast to what one would think on the basis of usual physical arguments, such as one can find in ref. 28.

In fact Ising-type behavior (after transition) in extended dynamical systems (as CMLs are) is an example of persistent space-time intermittency, and it appears to be the result of some subtle interplay between the local production of chaos and the spatial diffusion, the processes that govern the dynamics of the class of coupled map lattices that we consider. The exact character of the bifurcations that lead to the transition from space-time chaos (which is proven to exist in such CML for small coupling[26, 27]) to the (partially) ordered states after bifurcation is still unclear.

Our results point out that coupled map lattices can have a richer variety of behavior than the lattice spin systems of statistical mechanics, and provide some of the (maybe simplest) examples of how Ising-type transitions can fail to appear in one-dimensional CMLs, though this important question needs more work to be fully clarified.

The task of providing rigorous proofs and of getting a better understanding of the exact mechanism of Ising-type and other chaos–order transitions in CMLs will be the subject of further studies.

ACKNOWLEDGMENTS

We are indebted to D. Huse and I. Miller for letting us know their results before publication. We thank also D. Huse, I. Miller, P. Hohenberg, B. Shraiman, and A. Vulpiani for fruitful discussions.

One of us (A. P.) thanks Pierre Picco for the hospitality at Centre de Physique Theorique, Marseille Luminy.

We are grateful to a referee who insisted on requiring more precise data, which led to more work, and to a better understanding of some crucial points.

The work of C. B., G. C., S. F., and A. P. was partially supported by CNR (GNFM) and MURST research funds. The work of L. A. B. was partially supported by NSF grant DMS-9303769.

REFERENCES

1. Ya. G. Sinai, ed., *Dynamical Systems*; in *Encyclopedia of Mathematics*, Vol. II (Springer-Verlag, Berlin, 1987).
2. R. Mañé, *Ergodic Theory and Differentiable Dynamics* (Springer-Verlag, Berlin, 1987).
3. D. Ruelle, *Elements of Differentiable Dynamics and Bifurcation Theory* (Academic Press, 1989).
4. J. Guckenheimer and P. Holmes, *Nonlinear Oscillations, Dynamical Systems and Bifurcations of Vector Fields* (Springer-Verlag, Berlin, 1983).

5. J. Hale, *Ordinary Differential Equations* (Krieger, Malebar, Florida, 1980).
6. J. P. Eckmann and D. Ruelle, Ergotic theory of chaos and strange attractors, *Rev. Mod. Phys.* **57**:617 (1985).
7. A. S. Monin and A. M. Yaglom, *Statistical Fluid Mechanics, Mechanics of Turbulence* (MIT Press, Cambridge, Massachusetts, 1971).
8. K. G. Batchelor, *An Introduction to Fluid Dynamics* (Cambridge University Press, Cambridge, 1967).
9. J. L. Lumley, Ed., *Whither Turbulence*? (Springer-Verlag, Berlin, 1990).
10. D. D. Joseph, *Stability of Fluid Motions, Vols. I and II* (Springer-Verlag, Berlin, 1976).
11. K. Kaneko, ed., *Theory and Applications of Coupled Map Lattices* (Wiley, New York, 1993).
12. V. S. L'vov *et al.* in *Nonlinear Dynamics and Turbulence*, G. I. Barenblatt *et al.*, eds. (Pitman, 1983).
13. L. A. Bunimovich and Ya. G. Sinai, Spacetime chaos in coupled map lattices, *Nonlinearity* **1**:491–516 (1988).
14. L. A. Bunimovich and Ya. G. Sinai, in *Theory and Applications of Coupled Map Lattices*, K. Kaneko, ed. (Wiley, New York, 1993).
15. V. L. Volevich, Kinetics of coupled map lattices, *Nonlinearity* **4**:37–48 (1991).
16. Ya. B. Pesin and Ya. G. Sinai, Space-time chaos in chains of weakly interacting hyperbolic mappings, in *Advances in Soviet Mathematics*, Vol. 3, Ya. G. Sinai, ed. (Harwood Academic, Chur, Switzerland, 1991).
17. G. Keller and M. Kunzle, Transfer operators for coupled map lattices, *Ergod. Theory Dynamic Syst.* **12**:297–318 (1992).
18. J. Bricmont and A. Kupiainen, Coupled analytic maps, Preprint (1994).
19. Ya. G. Sinai, Gibbs measures in ergodic theory, *Russ. Math. Surv.* **27**:21–64 (1972).
20. D. Ruelle, *Thermodynamic Formalism* (Addison-Wesley, Reading, Massachusetts, 1978).
21. L. A. Bunimovich, A. Lambert, and R. Lima, The emergence of coherent structures in coupled map lattices, *J. Stat. Phys.* **61**(1/2):253–262 (1990).
22. A. I. Rakhmanov and N. K. Rakhmanova, On one dynamic system with discrete time, Preprint of the Keldysh Institute for Applied Mathematics, Moscow (1990).
23. C. Giberti and C. Vernia, On the presence of normally attracting manifolds containing periodic or quasi periodic orbits in coupled map lattices, *Int. J. Bifurcation Chaos*, to appear.
24. C. Giberti and C. Vernia, Normally attracting manifolds and periodic behavior in 1-*D* and 2-*D* coupled map lattices, *Chaos*, to appear.
25. P. Grassberger and T. Schreiber, Phase transitions in coupled map lattices, *Physica D* **50**:177–186 (1991).
26. V. Afraimovich and L. A. Bunimovich, Simplest structures in coupled map lattices and their stability, *Random Computational Dynamics* **1**:423–444 (1993).
27. L. A. Bunimovich and E. A. Carlen, On the problem of stability in lattice dynamical systems, *J. Differential Equations*, to appear.
28. J. Miller and D. Huse, Macroscopic equilibrium from microscopic irreversibility in a chaotic coupled-map lattice, *Phys. Rev. E* **48**:2528–2535 (1993).
29. V. S. Afraimovich, On the Lyapunov dimension of invariant sets in a model of an active medium, *Selecta Math. Sov.* **10** (1991).
30. S. Isola, A. Politi, S. Ruffo, and A. Torcini, Lyapunov spectra of coupled map lattices, *Phys. Lett.* **143 A**:365–369 (1990).
31. K. Kaneko, Pattern dynamics in spatiotemporal chaos, *Physica D* **34**:1–41 (1989).
32. R. Livi, A. Politi, S. Ruffo, and A. Vulpiani, Lyapunov exponents in high dimensional symplectic maps, *J. Stat. Phys.* **46**:147–158 (1987).